

Up-regulation of PPAR γ , heat shock protein-27 and -72 by naringin attenuates insulin resistance, β -cell dysfunction, hepatic steatosis and kidney damage in a rat model of type 2 diabetes

Ashok Kumar Sharma¹, Saurabh Bharti¹, Shreesh Ojha¹, Jagriti Bhatia¹, Narender Kumar², Ruma Ray², Santosh Kumari³ and Dharamvir Singh Arya^{1*}

¹Department of Pharmacology, Cardiovascular and Diabetes Research Laboratory, All India Institute of Medical Sciences, New Delhi 110029, India

²Department of Pathology, All India Institute of Medical Sciences, New Delhi 110029, India

³Department of Plant Physiology, Indian Agricultural Research Institute, Pusa, New Delhi 110012, India

(Received 2 February 2011 – Revised 15 March 2011 – Accepted 15 March 2011 – First published online 21 June 2011)

Abstract

Naringin, a bioflavonoid isolated from grapefruit, is well known to possess lipid-lowering and insulin-like properties. Therefore, we assessed whether naringin treatment ameliorates insulin resistance (IR), β -cell dysfunction, hepatic steatosis and kidney damage in high-fat diet (HFD)–streptozotocin (STZ)-induced type 2 diabetic rats. Wistar albino male rats were fed a HFD (55% energy from fat and 2% cholesterol) to develop IR and on the 10th day injected with a low dose of streptozotocin (40 mg/kg, intraperitoneal (ip)) to induce type 2 diabetes. After confirmation of hyperglycaemia (>13.89 mmol/l) on the 14th day, different doses of naringin (25, 50 and 100 mg/kg per d) and rosiglitazone (5 mg/kg per d) were administered orally for the next 28 d while being maintained on the HFD. Naringin significantly decreased IR, hyperinsulinaemia, hyperglycaemia, dyslipidaemia, TNF- α , IL-6, C-reactive protein and concomitantly increased adiponectin and β -cell function in a dose-dependent manner. Increased thiobarbituric acid-reactive substances and decreased antioxidant enzyme activities in the serum and tissues of diabetic rats were also normalised. Moreover, naringin robustly increased PPAR γ expression in liver and kidney; phosphorylated tyrosine insulin receptor substrate 1 in liver; and stress proteins heat shock protein (HSP)-27 and HSP-72 in pancreas, liver and kidney. In contrast, NF- κ B expression in these tissues along with sterol regulatory element binding protein-1c and liver X receptor- expressions in liver were significantly diminished. In addition, microscopic observations validated that naringin effectively rescues β -cells, hepatocytes and kidney from HFD-STZ-mediated oxidative damage and pathological alterations. Thus, this seminal study provides cogent evidence that naringin ameliorates IR, dyslipidaemia, β -cell dysfunction, hepatic steatosis and kidney damage in type 2 diabetic rats by partly regulating oxidative stress, inflammation and dysregulated adipocytokines production through up-regulation of PPAR γ , HSP-27 and HSP-72.

Key words: Insulin resistance: Type 2 diabetes: Naringin: Heat shock proteins: PPAR γ

Diabetes mellitus remains an important cause of morbidity and mortality, has reached burgeoning epidemic proportions affecting about 285 million individuals in 2010 and it is estimated that the number of diabetic individuals will be increased by 54% till 2030⁽¹⁾. More than 90% of diabetic individuals have type 2 diabetes mellitus (T2DM), a consequence of a high-fat diet, sedentary lifestyle and genetic predisposition, often diagnosed after metabolic dysfunction has taken hold of multiple organ systems^(1,2). The myriad of disorders

linked with T2DM includes oxidative stress, inflammation, insulin resistance (IR), insulin deficiency due to β -cell failure, dyslipidaemia, hepatic steatosis, diabetic nephropathy and retinopathy^(3–5). Emerging data indicate that chronic subacute inflammation in T2DM manifested as dysregulated production of C-reactive protein (CRP), TNF- α , IL-6 and adiponectin plays a crucial role in IR^(2,6).

Tragically, the present therapy for diabetes including insulin and various oral anti-diabetic agents is frequently constrained

Abbreviations: CRP, C-reactive protein; ER, endoplasmic reticulum; GSH + Px, glutathione peroxidase; HFD, high-fat diet; HOMA, homoeostasis model assessment; HSP, heat shock protein; ip, intraperitoneal; IR, insulin resistance; IRS1, insulin receptor substrate 1; LXR α , liver X receptor- α ; P-IRS1, phosphorylated tyrosine 612 IRS1; SOD, superoxide dismutase; SREBP-1c, sterol regulatory element binding protein-1c; STZ, streptozotocin; T2DM, type 2 diabetes mellitus; TBARS, thiobarbituric acid-reactive substances; TC, total cholesterol.

* **Corresponding author:** D. S. Arya, fax +91 11 26584121, email dsarya16@hotmail.com

by safety, tolerability, oedema, weight gain, lactic acidosis and gastrointestinal intolerance⁽⁷⁾. Moreover, drugs from natural resources are usually considered safe, and accessible interventions are becoming more popular in the treatment of several disorders including diabetes⁽⁸⁾. Human diets of plant origin contain polyphenols, phytosterols, phyto-oestrogens, phytates and PUFA, and so on. Among them, naringin, a polyphenol and naturally occurring bioflavonoid in grapefruits and oranges, has been reported to possess antioxidant, anti-diabetic, lipid-lowering, anti-atherogenic and anti-inflammatory activities^(9–12).

Interestingly, it is well known that activation of PPAR γ , a nuclear receptor, can exert anti-inflammatory and antioxidant effects in several cell types including pancreatic β -cells, hepatocytes and glomeruli^(13,14). Therefore, PPAR γ ligands can offer a therapeutic intervention in modifying diabetes and the metabolic syndrome⁽¹⁴⁾. Besides, heat shock proteins (HSP) are powerful antioxidant and anti-inflammatory proteins that protect cells against many acute and chronic stressful conditions^(15–17). Furthermore, activation of PPAR γ and HSP prevents IR and complications of diabetes by inhibiting NF- κ B and c-jun amino terminal kinase activation^(13–17). Recently, Jung *et al.*⁽¹¹⁾ reported that naringin up-regulated the PPAR γ receptor; therefore, we hypothesise that it might ameliorate IR, diabetes and its associated complications in high-fat diet (HFD)–streptozotocin (STZ)-induced type 2 diabetic rats.

With this background, for the first time, the present study was undertaken to investigate the effects of naringin on glucose homeostasis, dyslipidaemia, hepatic steatosis and kidney damage in HFD-STZ-induced type 2 diabetic rats. To delineate the mechanisms whereby naringin exerts its insulin-sensitising and anti-diabetic activity in diabetic rats, we evaluated oxidative stress, CRP, adipocytokines, as well as protein expression of PPAR γ , HSP-27, HSP-72, NF- κ B, sterol regulatory element binding protein-1c (SREBP-1c), liver X receptor α (LXR α) and phosphorylated tyrosine and total insulin receptor substrate. Morphological examinations of pancreas, liver and kidneys were also performed to further substantiate the beneficial effect of naringin on pathological alteration induced by HFD-STZ treatment. In the present study, the efficacy of naringin was compared with that of the PPAR γ agonist rosiglitazone, which is an insulin-sensitising anti-diabetic drug.

Materials and methods

Animals and diet

The experimental protocol was approved by the Institutional Animal Ethics Committee and conformed to the Indian National Science Academy guidelines for the use and care of experimental animals in research. Normal rat chow (55% carbohydrate, 24% protein, 6% ash, 5.0% moisture, 5% fat, 4% fibre, 0.6% Ca and 0.4% P, w/w) and a high-fat diet (25% coconut oil, 2% cholesterol and 73% normal rat chow; provides 55% of the animal's energy as fat) were used and animals were allowed access to food and water *ad libitum*. Wistar albino male rats (170–200 g, n 72) were adapted to

the experimental conditions at $25 \pm 5^\circ\text{C}$ with a relative humidity of $60 \pm 5\%$ on a light–dark cycle of 12–12 h for 1 week.

Drug and chemicals

Naringin and STZ were purchased from Sigma Chemicals (St Louis, MO, USA). Rosiglitazone was obtained as a gift sample from Zydus Cadila (Ahmedabad, Gujarat, India). Rat TNF- α (Diacclone Telpel Company, France), IL-6, high-sensitivity CRP (Bender MedSystems, Inc., Vienna, Austria), adiponectin (Linco Research, Inc., St Charles, MO, USA) and insulin (Mecrodia AB, Uppsala, Sweden) ELISA Kits were used. The kits for blood glucose, NEFA and lipid profile were purchased from Logotech Private Limited (New Delhi, India). All primary and secondary antibodies were procured from Santa Cruz Biotechnology, Inc. (Santa Cruz, CA, USA) except HSP-72 primary antibody (Stressgen, Plymouth Meeting, PA, USA).

Induction of type 2 diabetes and dyslipidaemia

Animals were assigned to either regular rat chow (normal control) or the HFD. After 10 d of the HFD, overnight-fasted (12 h) rats were injected a single injection of freshly prepared STZ (40 mg/kg, intraperitoneally (ip), in 0.1 M-citrate–phosphate buffer, pH 4.5). The development of hyperglycaemia in rats was confirmed by estimation of fasting serum glucose 72 h after STZ injection. Rats with fasting serum glucose level above 13.89 mmol/l were considered diabetic and recruited in the study. The schematic diagram of the experimental protocol is given in Fig. 1.

Experimental design

The rats were randomly divided into six groups comprising of twelve animals in each and were treated with naringin and rosiglitazone by oral administration for 28 d while being maintained on the HFD. Group I, normal control (normoglycaemic rats fed with normal diet only), group II, diabetic control (diabetic rats fed with HFD), groups III–V, diabetes–HFD rats, were administered naringin at 25, 50 and 100 mg/kg per d, by mouth respectively⁽¹²⁾. Group VI, Diabetes–HFD rats, were administered rosiglitazone at 5 mg/kg per d.

At the end of the experiment, blood samples were withdrawn from the tail vein of overnight-fasted rats. Subsequently, a glucose tolerance test and insulin tolerance tests were performed. The animals were then killed with an overdose of sodium pentobarbitone (150 mg/kg, ip) and their pancreas, liver and kidney were removed and processed for biochemical and microscopic examination. Serum was separated by centrifugation (Biofuge;

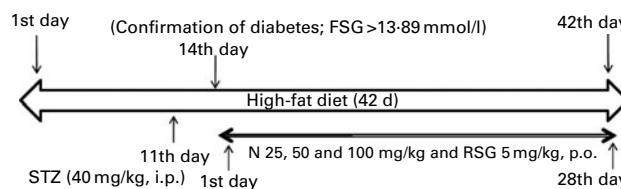


Fig. 1. Schematic diagram of experimental protocol. FSG, fasting serum glucose; N, naringin; RSG, rosiglitazone; p.o., by mouth; i.p., intraperitoneally.

Heraeus, Germany) at 3000 g for 5 min and analysed for glucose, total cholesterol (TC), TAG, LDL-C, HDL-C, insulin, adiponectin, IL-6, CRP and TNF- α .

Glucose tolerance and insulin tolerance tests

Overnight-fasted rats were administered glucose (1 g/kg, ip) and subsequently blood was withdrawn from the tail to estimate blood glucose levels at -1, 30, 60, 120 and 180 min using a glucometer (OneTouch; Johnson and Johnson, New Brunswick, NJ, USA). Once blood glucose levels returned to baseline, an insulin tolerance test was performed with insulin (Humulin, 0.5 units/kg, ip; Eli Lilly, India) and blood glucose levels were determined at -1, 15, 30, 45 and 60 min⁽⁵⁾.

Serum glucose, NEFA and lipid profile

Serum glucose, NEFA and lipid profiles (TC, TAG, LDL-C and HDL-C) were estimated spectrophotometrically using commercial kits.

Serum insulin, IL-6, C-reactive protein, TNF- α and adiponectin

Serum insulin, IL-6, CRP, TNF- α and adiponectin levels were measured by ELISA kits following the manufacturers' instructions.

Insulin resistance and β -cell function

Homeostasis model assessment (HOMA) of IR (HOMA-IR) and HOMA of β -cell function (HOMA-B) were calculated by the HOMA method using the following equations⁽¹⁸⁾:

$$\text{IR (HOMA-IR)} = (\text{fasting glucose (mmol/l)} \times \text{fasting insulin } (\mu\text{IU/ml})) / 22.5, \text{ and } \beta\text{-cell function (HOMA-B)} = (20 \times \text{fasting insulin } (\mu\text{IU/ml})) / (\text{fasting glucose (mmol/l)} - 3.5).$$

Thiobarbituric acid-reactive substances, superoxide dismutase and glutathione peroxidase activities

For measuring thiobarbituric acid-reactive substances (TBARS), aliquots of 10% homogenate of pancreas, liver and kidney were prepared in ice-cold phosphate buffer (0.1 M, pH 7.4). To this tissue homogenate, 8.1% SDS (0.2 ml), 20% acetic acid (1.5 ml) and 0.8% thiobarbituric acid (1.5 ml) were added and heated for 60 min in a boiling water bath. After cooling, the pink complex was extracted with 5 ml butanol-pyridine (15:1) mixture. Finally, absorbance of the organic layer was observed at 532 nm (Specord 200; Jena, Germany) and plotted against a standard graph and expressed as mmol/g tissue⁽¹⁹⁾.

Tissue homogenate so obtained was centrifuged (Biofuge; Heraeus, Germany) at 3000 g for 15 min at 4°C and the supernatant was collected to assess superoxide dismutase (SOD), glutathione peroxidase (GSH-Px) and protein. For SOD, 100 μ l supernatant, 2.95 ml phosphate buffer (0.1 M, pH 8.4) and 50 μ l pyrogallol (7.5 mM) were added and the change in absorbance was recorded at an interval of 60 s for 2 min at 420 nm. One unit of enzyme activity was defined as the amount of

Table 1. Biochemical and histological findings in different experimental groups at the end of the study (Mean values with their standard deviations; n 12)

Parameters	Normal control		Diabetic control		Diabetic + N25		Diabetic + N50		Diabetic + N100		Diabetic + RSG5	
	Mean	SD	Mean	SD	Mean	SD	Mean	SD	Mean	SD	Mean	SD
Body weight (g)	231.5	10.6	217.8	14.8	218.6	10.1	225.4	11.2	222.7	13.1	229.5	9.8
Serum glucose (mmol/l)												
Initial (day 1)	4.6	0.5	15.7	1.7	15.8	1.3	16.5	1.1	16.1	2.2	16.3	2.7
Final (day 28)	5.0	0.3	16.7**	2.2	14.3	1.4	10.1†††	1.6	8.3†††	1.5	8.6†††	1.9
Insulin (pmol/l)	77.0	5.9	123.2**	7.1	110.9	5.4††	94.7†††	2.4	88.2†††	4.0	89.6†††	4.9
HOMA-IR	2.46	0.14	12.54**	2.13	10.07	1.56†	6.12†††	1.19	4.64†††	0.63	4.92†††	1.10
HOMA-B	145.9	10.4	26.7**	3.5	34.9	5.0	44.3	10.1	58.7†	12.9	56.8†	10.9
TNF- α (pg/ml)	14.8	3.5	97.5**	4.1	86.1	6.4	52.5†††	7.5	41.3†††	5.1	44.6†††	2.7
IL-6 (pg/ml)	22.8	5.1	56.3**	8.7	50.5	7.8	41.8†	5.6	29.4†††	6.0	31.1†††	4.5
CRP (mg/l)	35	7	136**	13	131	15	102††	17	73†††	14	75†††	1.6
Adiponectin (μ g/ml)	32.4	1.5	18.6**	1.2	22.7	1.8	25.3††	0.9	28.5†††	1.7	29.0†††	1.2
Islet area (μm^2)	3237	582	1215**	296	1523	352	2389†††	638	2953†††	525	2820†††	602
Glomerular sclerosis (%)	3	1	9.45**	1.5	8.13	1.86	6.85	2.16	4.15†††	1.3	4.98†††	1.73
Glomerular area (μm^2)	18083	2045	16104	2195	16709	2345	17801	2065	18065	2278	18049	2132

HOMA-IR, homeostasis model assessment of IR; HOMA-B, homeostasis model assessment of β -cell function; CRP, C-reactive protein. Mean values were significantly different from those of the normal control: ** $P < 0.001$, *** $P < 0.001$ by one-way ANOVA followed by Bonferroni post hoc test. Mean values were significantly different from those of the diabetic control: † $P < 0.05$, †† $P < 0.01$, ††† $P < 0.001$ by one-way ANOVA followed by Bonferroni post hoc test.

enzyme required to produce 50% inhibition of pyrogallol auto-oxidation under the assay conditions and expressed as U/mg protein⁽²⁰⁾.

For GSH-Px, 100 μ l supernatant were added to the reaction mixture containing 1 mM-glutathione reductase in a 0.1 M-Tris-HCL (pH 7.2). The reaction was started by adding 2.5 mM-hydrogen peroxide and the absorbance was measured for 1 min at 340 nm. A molar extinction coefficient of 6.22 per mMcm was used to determine the activity and was expressed as U/mg protein⁽²¹⁾.

Further, protein estimation was carried out by adding 10 μ l tissue supernatant to 100 μ l of 1 M-NaOH and 1 ml Bradford reagent (Sigma Chemicals). The solution so obtained was vortexed and the absorbance was recorded at 595 nm⁽²²⁾. Protein content was determined from a standard curve using known concentrations of bovine serum albumin (Sigma Chemicals). Similarly, following the above-mentioned methods, we assessed TBARS, SOD, GSH-Px and total protein in the serum.

Western blot analysis

Protein samples (50 μ g) were separated by 12% SDS-PAGE, transferred to a nitrocellulose (MDI, Ambala, Haryana, India)

membrane that was blocked for 1 h with 5% (w/v) dry milk in Tris-buffered saline, and incubated overnight at 4°C with the mouse monoclonal primary antibody. The primary antibodies used were as follows: PPAR γ (1:2000), insulin receptor substrate 1 (IRS1; 1:1000), phosphorylated tyrosine 612 IRS1 (P-IRS1; Tyr162, 1:1000), HSP-27 (1:1500), HSP-72 (1:1500) and β -actin (1:2000). The primary antibody was detected with horseradish peroxidase-conjugated goat anti-mouse secondary antibody (1:10 000) and Bio-Rad Protein Assay Reagent, and visualised by Bio-Rad Quantity One software (release 4.4.0; Bio-Rad, Hercules, CA, USA).

Histopathological examination

Formaldehyde (10%)-fixed pancreas, liver and kidney tissues were embedded in paraffin, and serial sections (3 μ m) were cut using a microtome (Leica RM 2125; Leica, Germany). Each section was stained with haematoxylin and eosin and at least ten fields per slide were observed under a light microscope (Nikon, Tokyo, Japan). Endocrine pancreatic damage was assessed by evaluating changes in islet shape, area, cell number and presence of inflammatory infiltrate. Liver histopathological changes were graded as described by Jang

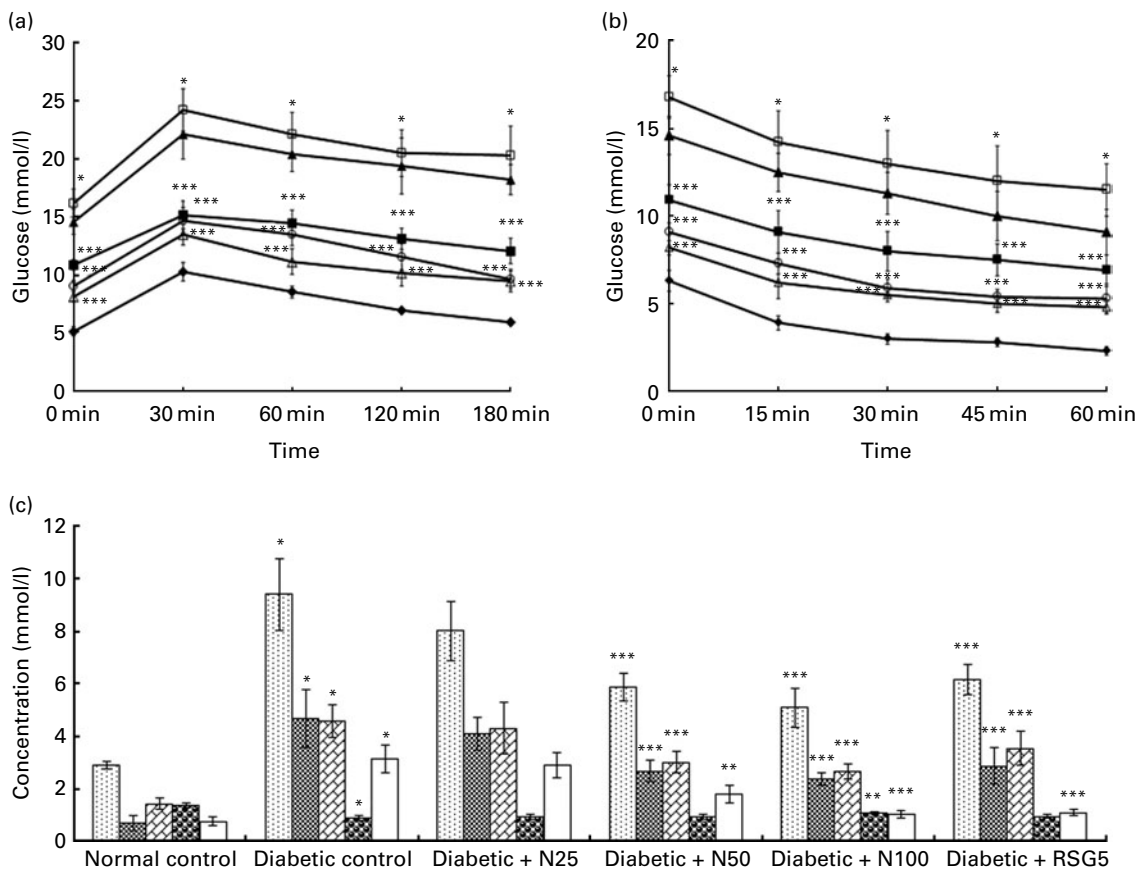


Fig. 2. (a) Glucose tolerance test (GTT); (b) insulin tolerance test (ITT); (c) serum lipid profile at the end of study in different experimental groups. Values are means, with their standard deviations represented by vertical bars (n 12). *Mean values were significantly different from those of the normal control ($P < 0.001$, one-way ANOVA followed by Bonferroni *post hoc* test). Mean values were significantly different from those of the diabetic control: ** $P < 0.01$, *** $P < 0.001$, one-way ANOVA followed by Bonferroni *post hoc* test. TC, total cholesterol. \bullet — \bullet , Normal control; \square — \square , diabetic control; \blacktriangle — \blacktriangle , diabetic + N25; \blacksquare — \blacksquare , diabetic + N50; \triangle — \triangle , diabetic + N100; \circ — \circ , diabetic + RSG5; \square , TC; \blacksquare , TAG; \square , LDL-C; \square , HDL-C; \square , NEFA.

et al.⁽²³⁾. The severity of kidney damage was evaluated in terms of morphological changes, such as hydropic changes in proximal convoluted tubules, glomerular sclerosis and widening of matrix. Sclerotic-glomeruli were ascertained by counting obsolescent glomeruli by a semi-quantitative scoring technique and reported as a percentage of approximately 100 glomeruli examined in each slide. Image-Pro Plus 4.0 software (Bethesda, MD, USA) was used to quantify change in pancreatic islets area and glomerular area. The pathologist performing histopathological evaluation was masked to the treatment protocol.

Transmission electron microscopy examination

Karnovsky's fixed tissues of pancreas and liver were washed in phosphate buffer (0.1 M, pH 7.4, 6°C) and post-fixed for 2 h in 1% osmium tetroxide in the same buffer at 4°C. The specimens were then dehydrated with graded acetone and embedded in araldite CY212 to make tissue blocks. Sections (70–80 nm) were cut by an ultra microtome (UltraCut E; Reichert, Austria) and stained with uranyl acetate and lead acetate and examined under a transmission electron microscope (Morgagni 268 D; Fei Co., the Netherlands) by a morphologist masked to the treatment protocol.

Statistical analysis

All results were expressed as the means and standard deviations⁽¹²⁾. Statistical analysis was performed using SPSS software package version 11.5.9 (San Francisco, CA, USA). The values were analysed by one-way ANOVA followed by Bonferroni *post hoc* test. $P < 0.05$ was considered statistically significant.

Results

Effect on body weight

Animals' body weight did not differ significantly between groups at the end of experiment (Table 1).

Effect on hyperglycaemia, hyperinsulinaemia, insulin resistance and β -cell function

Serum glucose, insulin and HOMA-IR levels were significantly elevated by 3.3-, 1.6- and 5.2-fold, respectively, in diabetic control rats compared with the normal controls (Table 1). Naringin dose dependently attenuated hyperglycaemia, hyperinsulinaemia and IR, so that the naringin 100 mg/kg group was not different from the standard drug rosiglitazone group (Table 1).

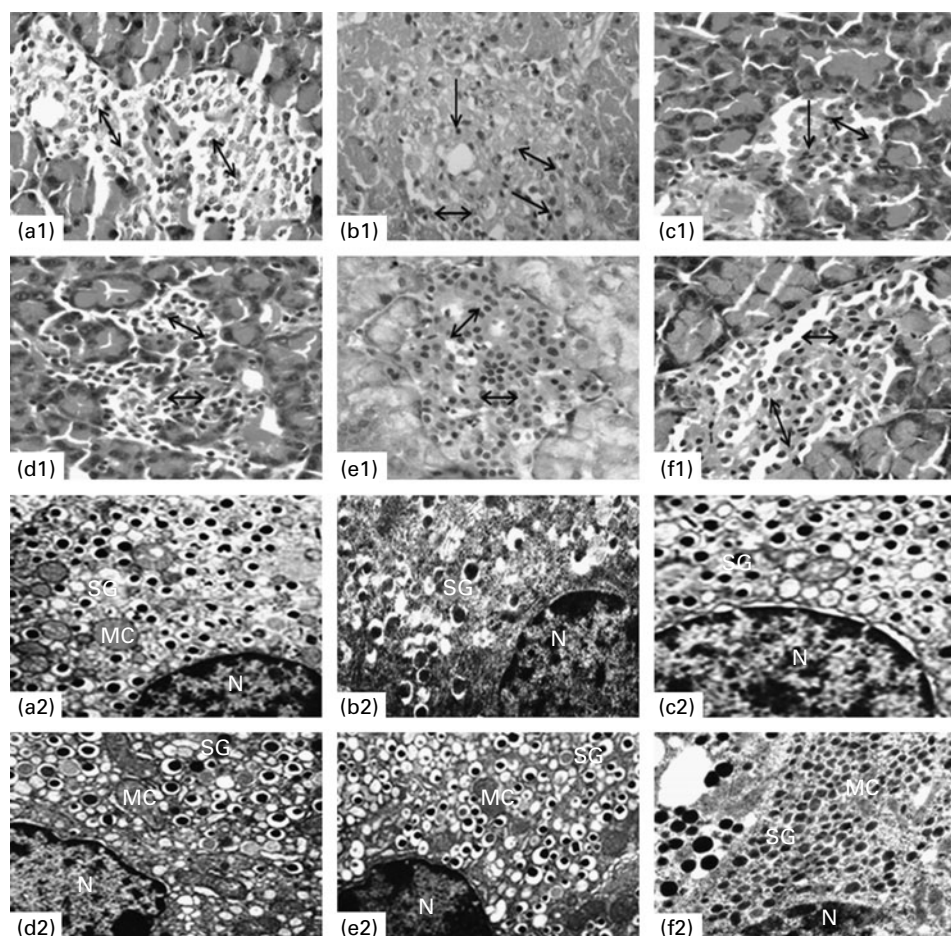


Fig. 3. Light microscopic study of pancreatic islet (a1–f1, 20 \times , scale bar 50 μ m) and electron microscopic study of β -cells (a2–f2, 4000 \times , scale bar 1 μ m) in different experimental groups. (a1 & a2) Normal control; (b1 & b2) diabetic control; (c1–e1 and c2–e2) Naringin 25, 50 and 100 mg/kg per d respectively; (f1 & f2) rosiglitazone treated. \leftrightarrow , β -cells; \leftarrow , inflammatory cells. N, nucleus; MC, mitochondria; SG, secretory granules.

Furthermore, as reflected in the results of the glucose tolerance test followed by the insulin tolerance test, diabetic control rats developed glucose intolerance and IR (Fig. 2a and b). In contrast, naringin at 50 and 100 mg/kg per d corrected impaired glucose utilisation and insulin insensitivity in diabetic rats (Fig. 2a and b). In addition, diabetic rats showed reduced (5.4-fold) β -cell function (HOMA-B), which was significantly ($P < 0.05$) improved by naringin at 100 mg/kg per d and rosiglitazone (Table 1).

Effect on dyslipidaemia and NEFA

Compared with normal controls, we found a 3.2-fold increase in serum TC, a 6.7-fold increase in TAG, a 3.2-fold increase in LDL-C and a 4.2-fold increase in NEFA in HFD-STZ-treated diabetic control rats (Fig. 2c). Naringin at 50 and 100 mg/kg significantly ($P < 0.001$) decreased TC (5.8 (SD 0.6); 5.0 (SD 0.7) *v.* 9.4 (SD 1.3) mmol/l), TAG (2.6 (SD 0.5); 2.3 (SD 0.3) *v.* 4.6 (SD 1.1) mmol/l), LDL-C (3.0 (SD 0.4); 2.6 (SD 0.3) *v.* 4.5 (SD 0.6) mmol/l) and NEFA (1.78 (SD 0.34) mmol/l; 1.02 (SD 0.15) *v.* 3.13 (SD 0.53) mmol/l) compared with diabetic control rats and the effect was more pronounced than with rosiglitazone. In addition, naringin at 100 mg/kg showed a significant ($P < 0.01$) increase in HDL-C (1.07 (SD 0.06) *v.* 0.86 (SD 0.09) mmol/l) compared with diabetic rats (Fig. 2c).

Effect on islets cell damage, islet atrophy and β -cell failure

Pancreatic histology of the normal control rats showed normal islet cell mass (Fig. 3a1); whereas diabetic control rats had severe damage on endocrine pancreas, including significant reduction of pancreatic islet area and atrophy of cells

(Fig. 3b1; Table 1). Middle and high doses of naringin repaired the injury of pancreatic islet cells and naringin at 100 mg/kg and rosiglitazone increased islet area to near-normal control levels (Fig. 3d1, 3e1; Table 1). Furthermore, on electron microscopic analysis compared with normal control (Fig. 3a2), β -cells from HFD-STZ-treated rats displayed a significantly distended endoplasmic reticulum (ER) and reduced insulin secretory granule numbers (Fig. 3b2). Treatment with naringin 100 mg/kg per d and rosiglitazone attenuated ER distension and preserved granule content, suggesting that naringin preserves β -cell function by maintaining an adequate pool of secretory granules (Fig. 3e2 and 3f2).

Effect on hydropic change of renal proximal convoluted tubules and glomerular sclerosis

In our study, diabetic control rats showed substantially hydropic change in proximal convoluted tubules and more widening of matrix (Fig. 4b) and administration of naringin at 100 mg/kg reversed these changes to near-normal control (Fig. 4e). Furthermore, naringin at 100 mg/kg significantly attenuated glomerular sclerosis, though there was no substantial difference in glomerular area between groups (Table 1).

Effect on protein expression of PPAR γ in liver and kidney, heat shock protein-27, -72 and NF- κ B in pancreas, liver and kidney, and insulin receptor substrate 1, phosphorylated tyrosine 612 IRS1 (Tyr162), liver X receptor and sterol regulatory element binding protein-1c in liver

HFD-STZ treatment decreased PPAR γ expression in liver and kidney, while naringin at 50, 100 mg/kg and rosiglitazone significantly ($P < 0.01$) increased PPAR γ expression (Fig. 5a).

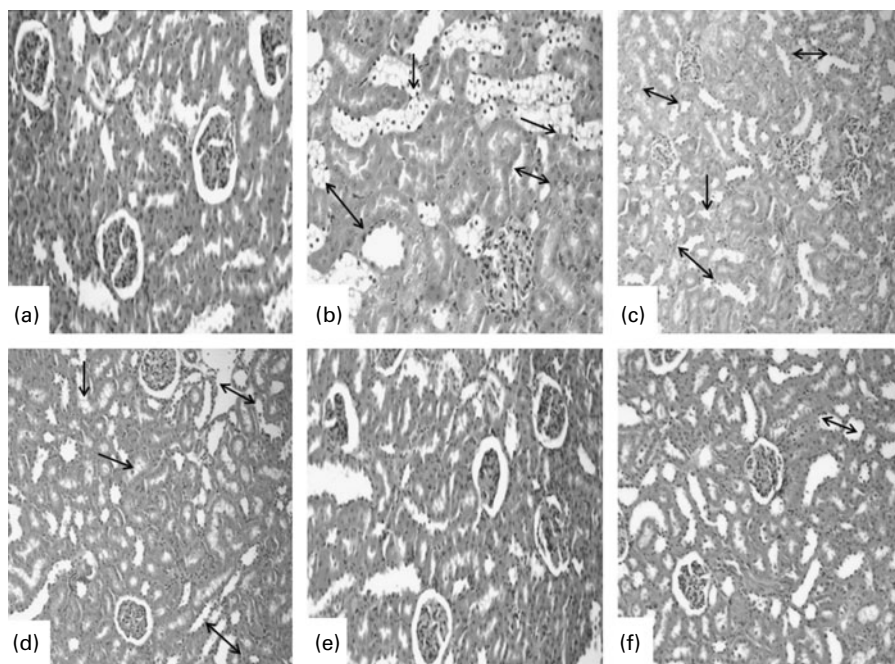


Fig. 4. Light microscopic study of kidney tissue in different experimental groups (a–f, scale bar 50 μ m). (a) Normal control (10 \times); (b) diabetic control (20 \times); (c–e) Naringin 25, 50 and 100 mg/kg per d (10 \times); (f) rosiglitazone treated (10 \times). \leftrightarrow , widening of matrix; \leftarrow , hydropic changes.

Further, the decreased IR in naringin (50 and 100 mg/kg)-treated rats was also associated with significantly increased P-IRS1 (Tyr162) expression without any change in total IRS1 expression in liver (Fig. 5b). Interestingly, in our study naringin treatment significantly increased the expression of HSP-72 (Fig. 5c) and HSP-27 (Fig. 5d), and the effect of naringin at 100 mg/kg was more pronounced than with rosiglitazone. Thus, it is very likely that one of the mechanisms by which naringin improves type 2 diabetes is by induction of HSP-72 and HSP-27.

To better understand the molecular mechanism underlying anti-inflammatory activity of naringin, we assessed NF-κB expression. Naringin treatment decreased the NF-κB protein expression in pancreas, liver and kidney dose dependently, which was found to be overexpressed in HFD-STZ-induced diabetic rats (Fig. 5e). Moreover, in our study observed hepatic steatosis in diabetic control rats was linked with increased expression of LXRα and SREBP-1c protein, which were significantly ($P < 0.001$) attenuated by naringin administered at 50 and 100 mg/kg (Fig. 5f).

Effect on serum TNF-α, IL-6, C-reactive protein and adiponectin

Serum TNF-α, IL-6 and CRP concentrations were significantly elevated by 6.6-, 2.5- and 3.8-fold, respectively, in diabetic control rats compared with normal controls (Table 1). In contrast, serum adiponectin levels were significantly ($P < 0.001$) decreased in diabetic control rats. Naringin reduced TNF-α, IL-6, CRP levels and increased adiponectin levels dose dependently, though the effect was significant at 50 and 100 mg/kg (Table 1).

Effect on thiobarbituric acid-reactive substances, superoxide dismutase and glutathione peroxidase

Table 2 represents the effect of naringin on the activities of enzymatic antioxidants and TBARS contents in serum, pancreas, liver and kidney. Diabetic control rats showed significant ($P < 0.001$) reductions in the activities of SOD, GSH-Px

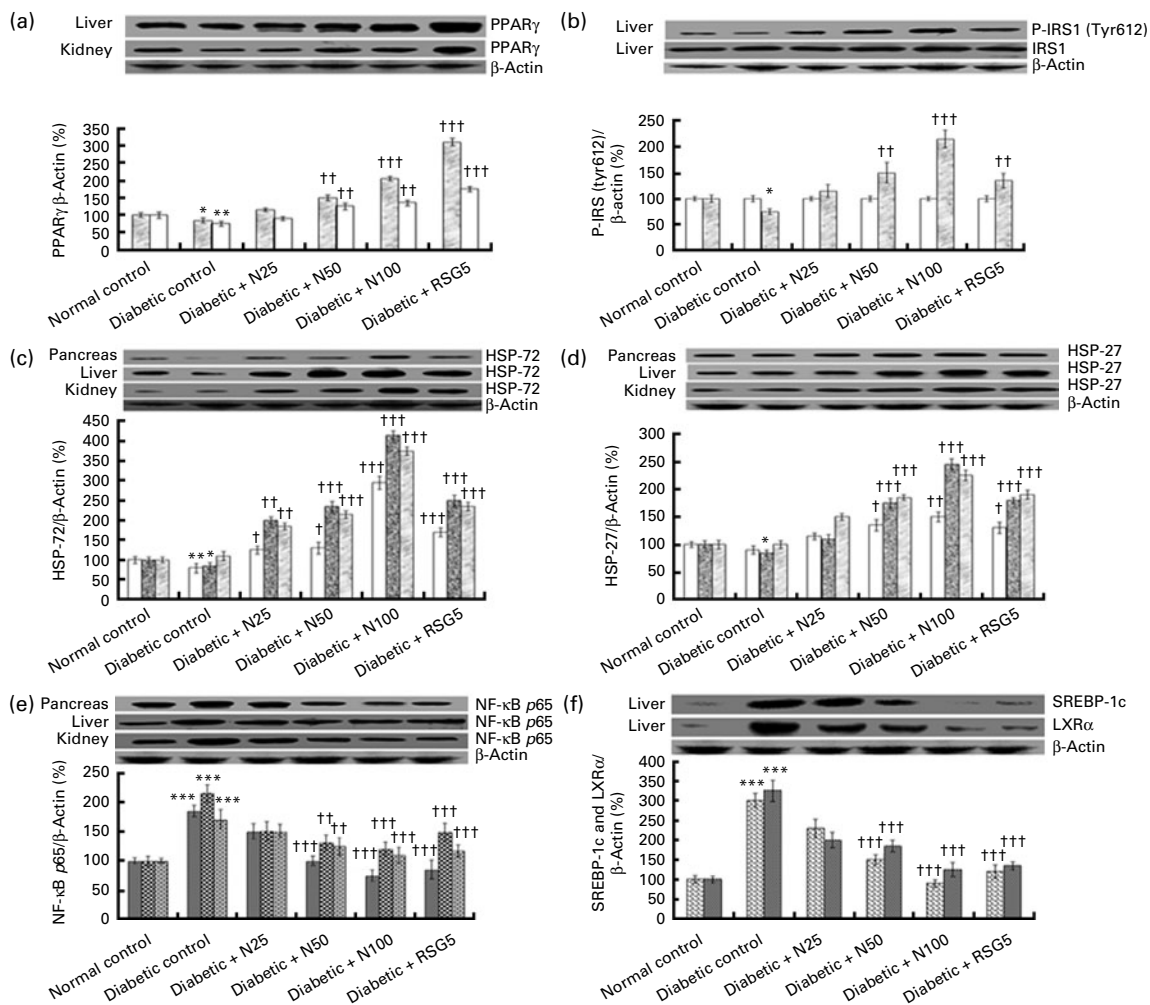


Fig. 5. Various protein expressions in different experimental groups. (a) PPAR γ expression in liver (□) and kidney (◻); (b) total insulin receptor substrate 1 (IRS1, ◻) and phosphorylated tyrosine 612 IRS1 (P-IRS1; Tyr612, ◻) expression in liver; (c) heat shock protein (HSP)-72 expression in pancreas (◻), liver (◻) and kidney (◻); (d) HSP-27 expression in pancreas (◻), liver (◻) and kidney (◻); (e) NF-κB expression in pancreas (◻), liver (◻) and kidney (◻); (f) sterol regulatory element binding protein-1c (SREBP-1c, ◻) and liver X receptor-α (LXRα, ◻) protein expression in liver. Data are expressed as a ratio of normal control value (set to 100%). Values are means, with their standard deviations represented by vertical bars ($n = 12$). Mean values were significantly different from those of the diet control: * $P < 0.05$, ** $P = 0.01$ by one-way ANOVA followed by Bonferroni *post hoc* test. Mean values were significantly different from those of the normal control: † $P < 0.05$, †† $P < 0.01$, ††† $P < 0.001$ by one-way ANOVA followed by Bonferroni *post hoc* test.

Table 2. Lipid peroxidation and antioxidant parameters in different experimental groups (Mean values with their standard deviations; n 12)

Parameters	Normal control		Diabetic control		Diabetic + N25		Diabetic + N50		Diabetic + N100		Diabetic + RSG5	
	Mean	SD	Mean	SD	Mean	SD	Mean	SD	Mean	SD	Mean	SD
TBARS (mmol/g)												
Serum	3.57	0.63	6.86*	1.03	5.44	1.49	4.36†††	0.86	3.98†††	0.32	4.13††	0.54
Pancreas	2.13	0.35	9.63*	0.74	8.21†	0.60	4.51††††	0.41	3.07††††	0.69	3.73††††	0.30
Liver	8.39	1.80	24.53*	3.08	20.92	5.63	16.37††††	2.06	12.04††††	1.42	12.87††††	2.04
Kidney	6.45	2.04	18.78*	2.74	17.26	3.07	12.89††††	1.12	9.07††††	1.07	12.17††††	1.23
SOD (U/mg protein)												
Serum	134.5	10.8	102.7*	12.5	113.2	8.6	118.9††	7.2	126.9††††	8.4	119.5†††	8.0
Pancreas	63.2	5.4	34.9*	7.4	41.0	5.7	48.5††	4.6	54.1††††	7.3	50.3††††	6.9
Liver	142.5	9.0	91.0*	10.3	102.4	11.5	12.4††	13.5	132.0††††	8.4	129.1††††	13.5
Kidney	125.6	7.1	87.2*	9.5	105.8†	12.6	114.8††††	10.7	118.2††††	9.1	117.4††††	15.4
GSH-Px (U/mg protein)												
Serum	14.02	2.45	10.45*	0.34	10.33	0.78	11.47†	0.46	12.71†††	0.67	12.80†††	5.9
Pancreas	1.64	0.22	0.76*	0.17	0.83	0.13	1.32††††	0.10	1.45††††	0.29	1.37††††	0.41
Liver	20.71	3.12	11.26*	2.43	13.02	4.05	15.14††	2.85	16.07†††	2.83	14.69†	2.11
Kidney	15.65	2.46	7.09*	3.04	8.35	2.06	10.77†††	3.10	12.89††††	1.83	12.08††††	2.23

TBARS, thiobarbituric acid-reactive substances; SOD, superoxide dismutase; GSH-Px, glutathione peroxidase. Mean values were significantly different from those of the normal control (* $P < 0.001$ by one-way ANOVA followed by Bonferroni post hoc test). Mean values were significantly different from those of the diabetic control: † $P < 0.05$, †† $P < 0.01$, ††† $P < 0.001$ by one-way ANOVA followed by Bonferroni post hoc test.

and an increase in the level of TBARS. When these diabetic rats were treated with naringin, we observed a significant ($P < 0.05$) decrease in TBARS and increase in SOD and GSH-Px activities in serum, pancreas, liver and kidney compared with diabetic control rats in a dose-dependent manner. However, naringin (100 mg/kg per d)-induced an increase in enzymatic antioxidant activity and a decrease in TBARS which were comparable with normal control and rosiglitazone groups.

Effect on hepatic steatosis

To assess the impact of naringin on changes in liver morphology in HFD-STZ-induced diabetic rats, we performed histopathological and ultrastructural analysis of liver tissue. Diabetic control rats showed increased inflammatory cells and a microvesicular hepatic steatosis on histopathological examination (Table 3). Furthermore, the electron microscopic analysis of hepatocyte revealed rarefied matrix, swelling of rough ER cisternae and mitochondria, fusion or loss of mitochondrial cristae, degranulation of rough ER and lipid accumulation in diabetic rats (data not shown). Naringin at 100 mg/kg per d reversed these pathological changes, and the effect was comparable with the normal control group (Table 3).

Discussion

In the present study, we have demonstrated that naringin ameliorates IR, β -cell dysfunction, dyslipidaemia, hepatic steatosis and pathological changes in kidney in HFD-STZ-induced type 2 diabetic rats in a dose-dependent manner. Furthermore, we established that this beneficial effect of naringin is because of attenuation of oxidative stress, CRP, ‘offensive’ adipocytokines TNF- α , IL-6 and correction of ‘defensive’ adipocytokine adiponectin. Importantly, improved glycaemic control with naringin is associated with increased PPAR γ , HSP-27, HSP-72 and decreased NF- κ B protein expression. Herein, we also demonstrated that attenuation of hepatic steatosis by naringin is linked with decreased hepatic LXR α and SREBP-1c protein expression. Our findings as well as those shown by other authors^(24–26) have demonstrated that animals, when fed with a HFD and injected with a low dose of STZ, display many characteristics of IR including hyperglycaemia, hyperinsulinaemia, impaired glucose tolerance test and insulin tolerance test, decreased β -cell function (HOMA-B), hyperlipidaemia, hepatic steatosis and kidney damage.

The primary basis of T2DM pathogenesis is unknown; however, there is a general agreement that IR followed by β -cell failure is a major event in the development of the disease⁽⁴⁾. Interestingly, in our study naringin treatment not only decreased hyperglycaemia, hyperinsulinaemia and IR, but also improved β -cell function and β -cell mass. Microscopic examination of endocrine pancreas revealed decreased β -cell mass, swelling of ER and diminished secretory granules in β -cells of HFD-STZ-treated rats indicating β -cell failure, which were mitigated by naringin. Our results suggest that reversal of IR and β -cell failure by naringin in HFD-STZ-induced diabetic rats is tightly associated with overexpression of PPAR γ , HSP-27 and HSP-72. The accumulated evidence

Table 3. Histological observations of hepatic tissue in experimental groups (*n* 12)

Groups	Swelling of hepatic cells	Fat accumulation	Displacement of nucleus	Loss of nucleus	Inflammatory cells
Normal control	–	–	–	–	–
Diabetic control	+++++	+++++	+++++	+++++	+++
Diabetic + N25	+++++	+++++	+++++	+++++	+++
Diabetic + N50	+++	+++	++	++	++
Diabetic + N100	+	+	+	+	+
Diabetic + RSG5	++	++	+	+	+

N25, naringin at 25 mg/kg per d; N50, naringin at 50 mg/kg per d; N100, naringin at 100 mg/kg per d; RSG5, rosiglitazone at 5 mg/kg per d; ++++++, high degree; +++++, severe; +++++, moderate; +++, fair; ++, mild; +, very mild; –, no changes in histology.

suggests that PPAR γ activation improves β -cell function and IR by decreasing NEFA and pro-inflammatory cytokines, consequently sparing skeletal muscle, liver and β -cells from detrimental metabolic effects of their high concentration^(4,13,14,27). Notably, our findings support the hypothesis that stress proteins play a significant role in the pathobiology of IR and T2DM, as expression of HSP-72 and HSP-27 decreased in diabetic rats, and their expression was increased along with the amelioration of diabetes in naringin- and rosiglitazone-treated rats. HSP-27 and HSP-72 are ubiquitous molecular chaperones induced in response to stressful conditions, such as inflammation, hypoxia, hyperglycaemia, oxidative stress, and preclude cell damage^(15–17,28). Recently, it has been proposed that HSP-72 protects against obesity-induced hyperglycaemia, hyperinsulinaemia and IR by inhibition of c-jun amino terminal kinase and inhibitor of κ B kinase⁽¹⁵⁾, which are critical inflammatory kinases in the development of IR and T2DM⁽²⁾. Similarly, various studies^(16,17) have reported that overexpression of HSP-72 and HSP-27 prevents the phosphorylation of inhibitor κ B, activation of *NF- κ B* and *TNF- α* gene transcription. Consistent with this, an interesting finding in our study was that naringin showed enhanced expression of HSP-27 and HSP-72 along with waning of *NF- κ B* expression, which might be a plausible mechanism involved in its better or similar response to a rosiglitazone even though comparatively lesser expression of PPAR γ .

In addition, abnormal production of adipocytokines, reactive oxygen species and advanced glycosylated end products in diabetes leads to *NF- κ B* activation and increased production of inflammatory mediators such as *TNF- α* and *IL-6*⁽²⁹⁾. Many aspects of biological processes, such as immune and inflammatory responses, as well as cell growth and apoptosis, are in part regulated by the *NF- κ B* system^(29,30). So we postulated that amelioration of β -cell damage and IR by naringin might be directly or indirectly associated with modulation of *NF- κ B* expression. Interestingly, in our study naringin administration dose-dependently attenuated *NF- κ B* expression and inflammatory mediators in diabetic rats, which shows its potential importance in metabolic diseases and T2DM. However, this inhibition of *NF- κ B* activity is probably a consequence of increased PPAR γ , HSP-72 and HSP-27 expression by naringin treatment^(4,13–17). Furthermore, IRS protein isoform, IRS1, is a decisive link in hepatic insulin signalling and increased serine/threonine phosphorylation in response to *TNF- α* , and various stresses in diabetes may be a key molecular lesion in hepatic IR⁽³¹⁾. In line with this assumption, our results indicate that the molecular mechanisms

underlying IR in diabetes may involve *TNF- α* -mediated activation of pro-inflammatory kinases (*NF- κ B*) and phosphatases that inhibit tyrosine phosphorylation of IRS1 and insulin action. Conversely, an enhanced level of P-IRS1 (Tyr162) and improved action of insulin by naringin seem to be a result of antagonism of *NF- κ B* activation, and this might be a consequence of increased PPAR γ , HSP-72 and HSP-27 expression with naringin^(4,13–17).

To elucidate the role of oxidative stress in HFD-STZ-treated diabetic rats and naringin-treated rats, we assessed oxidative/antioxidant status by measuring reactive oxygen species-induced products of lipid peroxidation (TBARS) and activity of SOD and GSH-Px in serum, pancreas, liver and kidney. Consistent with previous studies^(24,26), we observed reductions in the activities of SOD and GSH-Px as well as increased TBARS in serum and tissues of diabetic rats. Similar to Kim *et al.*⁽¹⁰⁾, our findings suggest the antioxidant activity of naringin increased the antioxidant enzymes and decreased TBARS levels in serum and tissues. Since increased reactive oxygen species production by mitochondria and ER leads to the activation of stress kinases, such as c-jun amino terminal kinase and inhibitor of κ B kinase, the two principal inflammatory pathways disrupt insulin action by decreasing P-IRS1 (Tyr162) and developing metabolic diseases^(2,3,32). Thus, drugs with antioxidant potential may attenuate T2DM. Furthermore, during the past decade many researchers have implicated increased oxidative stress as the major culprit in diabetes pathogenesis leading to dysregulated production of adipocytokines and acute-phase reactants^(2,3,31). Naringin treatment reduced circulating markers of chronic subacute inflammation, such as CRP, *TNF- α* and *IL-6*, that promote IR and at the same time increased adiponectin, which has insulin-sensitising activity. We speculate that naringin inhibits dysregulated production of adipocytokines and CRP in HFD-STZ-induced diabetic rats by decreasing oxidative stress and by modulation of PPAR γ , HSP-27, HSP-72 and *NF- κ B* protein expression^(13–17,30).

In our study diabetic rats showed markedly increased NEFA, TAG, TC, LDL-C and diminution in HDL-C. IR leads to decreased apoB100 intracellular degradation, resulting in increased VLDLapoB production and secretion⁽⁵⁾, which subsequently causes increased LDL-C and decreased HDL-C⁽³³⁾. Further, this increased dyslipidaemia in diabetic rats was also associated with microvesicular hepatic steatosis, swelling of ER and mitochondria in hepatocytes, which resembles fatty hepatic lesions observed in human patients with T2DM. Hepatic steatosis that often accompanies diabetes may be a consequence of hyperinsulinaemia and IR causing increased

expression of LXR α and SREBP-1c, thereby decreased NEFA oxidation and augmented lipogenesis in hepatocytes⁽⁵⁾. Even increased oxidative stress, serum NEFA and TNF- α in diabetic rats have also been reported to be crucially linked with hepatic steatosis^(23,26,31). As such, the present results raise the possibility that the beneficial effect of naringin on dyslipidaemia and hepatic steatosis may be partly mediated through the modulation of PPAR γ , HSP-27, HSP-72 and NF- κ B expression, which in turn leads to decreased LXR α and SREBP-1c activation, and consequently inhibition of lipogenic enzymes synthesis, lipogenesis and fat accumulation in hepatocytes^(5,13–15). Recently, many studies have suggested that naringin lowers the plasma and hepatic lipid levels by suppression of hepatic fatty acid synthase, glucose-6-phosphate dehydrogenase, HMG-CoA reductase activity, acyl CoA/cholesterol acyltransferase activities and by increasing faecal fat^(10,11).

Data presented in this study also add to the evidence that HFD-STZ treatment produces pronounced kidney lesions in rats because of associated hyperinsulinaemia, hyperlipidaemia, hyperglycaemia and increased oxidative stress⁽²⁴⁾. However, naringin prevented these pathological alterations due to its insulin-sensitising, anti-inflammatory, anti-dyslipidaemic and antioxidant activity. Herein, we also demonstrated that the mechanism for such an outcome is modulation of PPAR γ , HSP-27, HSP-72 and NF- κ B protein expression by naringin in kidney tissue^(13,16,17).

Thus in our study, naringin exerts various pharmacological effects in HFD-STZ-induced type 2 diabetic rats. Concerning its toxic effects, it is reported that naringin is safe and produced no lethality at a very high dose (5000 mg/kg, by mouth) in mice⁽³⁴⁾. Moreover, Lambev *et al.*⁽³⁵⁾ demonstrated that LD50 of naringin by the ip route in the rat and guinea pig is 2000 mg/kg. One major drawback associated with this flavanone glycoside is inhibition as well as the down-regulation of drug-metabolising cytochrome P450 enzymes such as CYP3A4 and CYP1A2, which may result in drug–drug interactions in diabetic individuals⁽³⁴⁾.

In summary, the present study finds naringin as effective as rosiglitazone and unravels the mechanism whereby naringin ameliorates IR, β -cell failure, hepatic steatosis and kidney damage in a rat model of T2DM. Up-regulation of PPAR γ , HSP-72, HSP-27 and suppression of NF- κ B by naringin prevent type 2 diabetes and its deleterious effects by attenuating oxidative stress, inflammation and dysregulated adipocytokine production in HFD-STZ-induced type 2 diabetic rats. Altogether, these findings indicate that naringin may be an effective therapeutic strategy for the treatment of diabetes and its associated complications; further experimental and clinical studies are required to explore the additional mechanisms and establish its clinical utility.

Acknowledgements

This study was supported by grant from an institutional funding agency, AIIMS, New Delhi, India. Special thanks to Deepak Sharma for his valuable technical assistance. A. K. S., S. B., S. O., J. B., S. K. and D. S. A. designed the research.

A. K. S. and S. B. performed the research. N. K. and R. R. analysed histopathological and electron microscopical changes. A. K. S., S. B., S. O., J. B., S. K. and D. S. A. analysed data and wrote the paper. All the authors read and approved the final submitted manuscript. None of the authors has any conflict of interest.

References

1. Shaw JE, Sicree RA & Zimmet PZ (2010) Global estimates of the prevalence of diabetes for 2010 and 2030. *Diabetes Res Clin Pract* **87**, 4–14.
2. Hotamisligil GS (2006) Inflammation and metabolic disorders. *Nature* **444**, 860–867.
3. Wellen KE & Hotamisligil GS (2005) Inflammation, stress, and diabetes. *J Clin Invest* **115**, 1111–1119.
4. Koning EJ, Bonner-Weir S & Rabelink TJ (2008) Preservation of beta-cell function by targeting beta-cell mass. *Trends Pharmacol Sci* **29**, 218–227.
5. Mulvihill EE, Allister EM, Sutherland BG, *et al.* (2009) Naringin prevents dyslipidemia, apolipoprotein B overproduction, and hyperinsulinemia in LDL receptor-null mice with diet-induced IR. *Diabetes* **58**, 2198–2210.
6. Furukawa S, Fujita T, Shimabukuro M, *et al.* (2004) Increased oxidative stress in obesity and its impact on metabolic syndrome. *J Clin Invest* **114**, 1752–1761.
7. Goldberg RB, Holman R & Drucker DJ (2008) Management of type 2 diabetes. *N Engl J Med* **358**, 293–297.
8. Nahas R & Moher M (2009) Complementary and alternative medicine for the treatment of type 2 diabetes. *Can Fam Physician* **55**, 591–596.
9. Jeon SM, Park YB & Choi MS (2004) Antihypercholesterolemic property of naringin alters plasma and tissue lipids, cholesterol regulating enzymes, fecal sterol and tissue morphology in rabbits. *Clin Nutr* **23**, 1025–1034.
10. Kim HJ, Oh GT, Park YB, *et al.* (2004) Naringin alters the cholesterol biosynthesis and antioxidant enzyme activities in LDL receptor-knockout mice under cholesterol fed condition. *Life Sci* **74**, 1621–1634.
11. Jung UJ, Lee MK, Park YB, *et al.* (2006) Effect of citrus flavonoids on lipid metabolism and glucose-regulating enzyme mRNA levels in type-2 diabetic mice. *Int J Biochem Cell Biol* **38**, 1134–1145.
12. Aggarwal A, Gaur V & Kumar A (2010) Nitric oxide mechanism in the protective effect of naringin against post-stroke depression (PSD) in mice. *Life Sci* **86**, 928–935.
13. Michalik L & Wahli W (2006) Involvement of PPAR nuclear receptors in tissue injury and wound repair. *J Clin Invest* **116**, 598–606.
14. Yki-Jarvinen H (2004) Thiazolidinediones. *N Engl J Med* **351**, 1106–1118.
15. Chung J, Nguyen AK, Henstridge DC, *et al.* (2008) HSP72 protects against obesity-induced IR. *Proc Natl Acad Sci USA* **105**, 1739–1744.
16. Meldrum KK, Burnett AL, Meng X, *et al.* (2003) Liposomal delivery of heat shock protein 72 into renal tubular cells blocks nuclear factor-kappaB activation, tumor necrosis factor-alpha production, and subsequent ischemia-induced apoptosis. *Circ Res* **92**, 293–299.
17. Garrido C, Bruey JM, Fromentin A, *et al.* (1999) HSP27 inhibits cytochrome *c*-dependent activation of procaspase-9. *FASEB J* **13**, 2061–2070.
18. Matthews DR, Hosker JP, Rudenski AS, *et al.* (1985) Homeostasis model assessment: IR and beta-cell function from

- fasting plasma glucose and insulin concentrations in man. *Diabetologia* **28**, 412–419.
19. Ohkawa H, Oohishi N & Yagi N (1979) Assay for lipid peroxides in animal tissues by thiobarbituric acid reaction. *Anal Biochem* **95**, 351–358.
 20. Marklund S & Marklund G (1974) Involvement of the superoxide anion radical in the autoxidation of pyrogallol and a convenient assay for superoxide dismutase. *Eur J Biochem* **47**, 469–474.
 21. Lawrence RA & Burk RF (1976) Glutathione peroxidase activity in selenium-deficient rat liver. *Biochem Biophys Res Commun* **71**, 952–958.
 22. Bradford MM (1976) A rapid and sensitive method for quantization of microgram quantities effects of age and caloric restriction. *Anal Biochem* **72**, 248–254.
 23. Jang A, Srinivasan P, Lee NY, *et al.* (2008) Comparison of hypolipidemic activity of synthetic gallic acid-linoleic acid ester with mixture of gallic acid and linoleic acid, gallic acid, and linoleic acid on high-fat diet induced obesity in C57BL/6Cr Slc mice. *Chem Biol Interact* **174**, 109–117.
 24. Danda RS, Habiba NM, Rincon-Choles H, *et al.* (2005) Kidney involvement in a nongenetic rat model of type 2 diabetes. *Kidney Int* **68**, 2562–2571.
 25. Srinivasan K, Viswanad B, Asrat L, *et al.* (2005) Combination of high-fat diet-fed and low-dose streptozotocin-treated rat: a model for type 2 diabetes and pharmacological screening. *Pharmacol Res* **52**, 313–320.
 26. Parveen K, Khan MR, Mujeeb M, *et al.* (2010) Protective effects of Pycnogenol on hyperglycemia-induced oxidative damage in the liver of type 2 diabetic rats. *Chem Biol Interact* **186**, 219–227.
 27. Serisier S, Leray V, Poudroux W, *et al.* (2008) Effects of green tea on insulin sensitivity, lipid profile and expression of PPARalpha and PPARgamma and their target genes in obese dogs. *Br J Nutr* **99**, 1208–1216.
 28. Morimoto RI (1993) Cells in stress: transcriptional activation of heat shock genes. *Science* **259**, 1409–1410.
 29. Martins de Lima-Salgado T, Coccuzzo Sampaio S, Fernanda Cury-Boaventura M, *et al.* (2011) Modulatory effect of fatty acids on fungicidal activity, respiratory burst and TNF- α and IL-6 production in J774 murine macrophages. *Br J Nutr* **14**, 1–7.
 30. Van den Berg R, Haenen GR, Van den Berg H, *et al.* (2001) Transcription factor NF-kappaB as a potential biomarker for oxidative stress. *Br J Nutr* **86**, Suppl. 1, S121–S127.
 31. Taniguchi CM, Ueki K & Kahn R (2005) Complementary roles of IRS-1 and IRS-2 in the hepatic regulation of metabolism. *J Clin Invest* **115**, 718–727.
 32. Ceriello A & Motz E (2004) Is oxidative stress the pathogenic mechanism underlying IR, diabetes, and cardiovascular disease? The common soil hypothesis revisited. *Arterioscler Thromb Vasc Biol* **24**, 816–823.
 33. Taskinen MR (2003) Diabetic dyslipidaemia: from basic research to clinical practice. *Diabetologia* **46**, 733–749.
 34. Alvarez-González I, Madrigal-Bujaidar E, Dorado V, *et al.* (2001) Inhibitory effect of naringin on the micronuclei induced by ifosfamide in mouse, and evaluation of its modulatory effect on the Cyp3a subfamily. *Mutat Res* **480-481**, 171–178.
 35. Lambev I, Krushkov I, Zheliazkov D, *et al.* (1980) Antiexudative effect of naringin in experimental pulmonary edema and peritonitis. *Eksp Med Morfol* **19**, 207–212.